

**WHY DO FIBONACCI NUMBERS APPEAR IN PATTERNS OF
GROWTH IN NATURE?
A MODEL FOR TISSUE RENEWAL BASED ON ASYMMETRIC CELL
DIVISION**

BRUCE M. BOMAN, THIEN-NAM DINH, KEITH DECKER, BROOKS EMERICK,
CHRISTOPHER RAYMOND, AND GILBERTO SCHLEINIGER

ABSTRACT. While many examples of Fibonacci numbers are found in phenotypic structures of plants and animals, the dynamic processes that generate these structures have not been fully elucidated. This raises the question: What biologic rules and mathematical laws that control the growth and renewal of tissues in multi-cellular organisms give rise to these patterns of Fibonacci numbers? In nature the growth and self-renewal of cell populations leads to generation of hierarchical patterns in tissues that resemble the pattern of population growth in rabbits, which is explained by the classic Fibonacci sequence. Consequently, we conjectured a similar process exists at the cellular scale that explains tissue renewal. Accordingly, we created a model (cell division type) for tissue development based on the biology of cell division that builds upon the cell maturation concept posed in the Spears and Bicknell-Johnson model (“mating”-like design) for asymmetric cell division. In our model cells divide asymmetrically to generate a mature and an immature cell. Model output on the number of cells generated over time fits specific Fibonacci p-number sequences depending on the maturation time. A computer code was created to display model output as branching tree diagrams as a function of time. These plots and tables of model output illustrate that specific patterns and ratios of immature to mature cells emerge over time based on the cell maturation period. Conclusion: Simple mathematical laws involving temporal and spatial rules for cell division begin to explain how Fibonacci numbers appear in patterns of growth in nature.

1. INTRODUCTION

Many examples of Fibonacci numbers are found in phenotypic structures of plants and animals. Indeed, Fibonacci numbers often appear in number of flower petals, spirals on a sunflower or nautilus shell, starfish, and fractions that appear in phyllotaxis [4, 18, 10]. In art, the aesthetic proportions of the human body as suggested by Leonardo da Vinci’s “Vitruvian Man” are described by ratios of Fibonacci numbers (termed the “golden ratio”) [5]. At lower levels of complexity, i.e. the intracellular and cellular scales, Fibonacci numbers have also been reported. For example, the organization of nucleic acid bases in the DNA sequence has an order (called the DNA SUPRA code) that follows Fibonacci numbering [6, 7]. The order of replication of DNA in cells also appears to follow the Fibonacci series [9]. Moreover, human epithelial cells that were grown in vitro showed a clonal growth pattern that followed the Fibonacci sequence [19, 20]. While these patterns of Fibonacci numbers appear at the molecular and cellular scales, it does not explain how Fibonacci numbers appear in patterns of growth at the organism scale.

We believed that the key to solving this problem was to investigate relevant dynamic processes that occur at the cellular scale because tissues are fluid, self-renewing, not stationary,

cellular systems. For example, in a seminal study, Spears and Bicknell-Johnson [15, 16] modeled the dynamics of cell division as an asymmetric process and discovered that the cell population expansion followed the Fibonacci numbers. In their study, asymmetric cell division was designed as a process that produces two progeny cells with different **temporal** (not phenotypic) properties. Based on this mechanism, their model output simulated the dynamic growth of cell populations and generation of hierarchical patterns found in tissues. Our current study builds upon this asymmetric cell division mechanism to understand the emergent-type laws that control the growth and renewal of tissues which give rise to these patterns of Fibonacci numbers in nature.

2. MODEL DESIGN

The dynamics of cell division were modeled as an asymmetric process based on the Spears and Bicknell-Johnson Model [15, 16]. In modeling asymmetric cell division, two progeny cells are produced with different temporal characteristics: one cell (mature) continues to undergo division every cycle and the other cell (immature) has a lag time for maturation before it undergoes division. Our current study builds upon this asymmetric mechanism by incorporating a design (cell division) for cell maturation (Figure 1) that fits the biology of cell division more closely than the “classic” Spears and Bicknell-Johnson (“mating”-like) design. In the “mating”-like design, the immature cell first becomes mature and then it divides (like a gestation period), but in our cell division the immature cell becomes mature upon reaching its first division (no gestation period). The cell maturation time is defined by the number of cell cycles between its initial production and its first division to produce a new immature cell. Mature cells continue to divide until they become wholly mature and no longer divide, and subsequently die (cell lifespan). Our study builds on this asymmetric cell division mechanism to understand the emergent-type laws that govern tissue renewal.

3. AN AGENT-BASED CODE FOR ASYMMETRIC CELL DIVISION

An agent-based code was also created for our model with the “agents” being the cells themselves, with cells having the counting properties of age and generation (the Netlogo code is available upon request). Based on the asymmetric division process, cells are distinguished as immature or mature. The age of a cell is defined by the number of time steps since its initial production. A cell divides if and only if it is a mature cell. The generation of a cell is the number of divisions removed from the original clonogenic cell (zeroth generation cell).

Three main properties define the cell’s behavioral dynamics: maturation-cycle (or age at maturation, the c value), whole-maturation time (n_{wm} or age at whole-maturation), and lifespan (L or age at death). In other words, these properties (c , n_{wm} , and L) specify the age at which cells change state: at age zero, a cell is immature; at age c , a cell becomes mature; at age n_{wm} , a cell becomes wholly-mature; at age L , the cell reaches the end of its life cycle and dies. The number of divisions undergone by any given cell can be determined by the following relationship: $\# \text{divisions} = n_{\text{wm}} - c$. For some model runs c and n_{wm} are programmed to decrease over time as a function of cell generation whereby $c = c_0 - k$, where $k = \text{generation}$, and $n_{\text{wm}} = n_{\text{wm},0} - k$ (c_0 and $n_{\text{wm},0}$ are initial constant values). Together, these intrinsic properties control the emergent dynamical behavior of a cell agent whereby generation, c , n_{wm} , and L remain constant during the lifetime of a cell, while age is continually incremented.

An initial objective was to define conditions that generate a steady-state structure. Steady-state is deemed to be a pattern which has a long-term cell population that is constant up to some small cyclic variation. If the c and n_{wm} values are controlled, then the overall growth rate

of the structure can be adjusted such that every mature cell under a steady-state condition only produces, on average, a single immature cell. In the code, the position of all cells is defined by their place within an implicit tree data structure that is rooted by the clonogenic cell's position. The c value of the clonogenic cell defines the pattern of the entire structure. The output was plotted as lineage trees to illustrate the numerical evolution of the model. The trees track all divisions that occur at each time step. Beginning with time zero and a single stem cell, each successive row of the tree indicates a new time step. Cells that remain alive between time steps are propagated downward to the next row of the tree and connected by a visual link. If a cell divides, then it is connected to both of its resulting halves in the next row. Output was also plotted as very large lineage trees at low resolution. In all lineage trees, the distance between horizontally adjacent nodes are equal. This indicates that the geometric width of the tree at any given height corresponds to the cell population size at that time.

4. RESULTS

Model output based on cell division as an asymmetric process showing that cell population expansion based on maturation delay (c value) follows the Fibonacci numbers (Table 1 & Figure 1).

$$F_n = F_{n-1} + F_{n-c} \tag{4.1}$$

A binomial equation for cell numbers in different generations where $n =$ time, $c =$ maturation delay, $k =$ generation, and $d =$ maturational age is given by Spears and Bicknell-Johnson Model [15, 16].

$$G_n = \sum_{k=0}^{\lfloor \frac{n+c-1}{c} \rfloor} \binom{n - (c-1)(k-1)}{k} = \sum_{k=0}^{\lfloor \frac{n}{c} \rfloor} \sum_{d=1}^{\min(c, n-kc+1)} \binom{n - k(c-1) - d + 1}{k} \tag{4.2}$$

where the floor function is defined as

$$\lfloor x \rfloor = \text{largest integer } \leq x .$$

Note that $\binom{n-(c-1)(k-1)}{k}$ is the number of cells in generation k at time n , while $\binom{n-k(c-1)-d+1}{k}$ is the number of cells in maturation age d ($1 \leq d \leq c$) and generation k at time n .

Cell numbers as a function of generation (Tables 2 & 3) are obtained from the formulas above.

The equation for the ratio of mature and immature cells based on c value (Tables 4 & 5) is

$$\frac{M}{I} = \left(\frac{I}{M+I} \right)^{c-1} = \left(\frac{1}{M/I+1} \right)^{c-1} . \tag{4.3}$$

If we let $x = M/I$ be the ratio of mature to immature cells, then x is a positive root of the polynomial equation (see Table 5)

$$x(x+1)^{c-1} - 1 = 0 .$$

Our computer code displays model output as branching tree diagrams as a function of time. Figure 2 shows the tree diagram generated from output of our agent-based computer code model for maturation time $c = 6$. Figure 3 shows the tree diagram generated from output involving maturation time $c = 6$ and when it is programmed to decrease over time as a function of cell generation ($n_{wm} = n_{wm,0} - k$) whereby $L = 50$ and $n_{wm,0} = 9$. These plots and tables of model output illustrate that specific patterns and ratios of immature to mature cells emerge over time based on the cell maturation period.

5. DISCUSSION

The sequences of number of cells generated by asymmetric cell division over time in our model are similar to known sequences in discrete mathematics. This is illustrated by sequences for $c = 1$ to $c = 6$ given in Table 1 that are related to recursive sequences previously described in both number theory and geometry [12, 11]. For example, the sequence for $c = 1$ consists of powers of 2, for $c = 2$ the Fibonacci numbers, and for $c = 3$ the Narayana's cows sequence. The limiting ratios of successive terms of these sequences are also related to previously reported constants. For example, for $c = 2$ the limiting ratio is the golden ratio, for $c = 5$ the limiting ratio corresponds to that for the Padovan sequence or Perrin sequence as well as the plastic constant. The limiting ratios for $c = 3$ to $c = 5$ have also been reported as Pisot-Vijayaraghavan numbers. In geometric terms, the limiting ratios of these sequences have also been reported for the Fibonacci p-numbers and are expressed as the division of line segments which has been termed "The Golden p-sections" [17]. While these sequences and their limiting ratios are well known in mathematics, analysis of their rate of growth to determine why Fibonacci numbers appear in patterns of growth in nature has not been extensively investigated.

Based on our model output from asymmetric cell division we begin to see how these recursive sequences might be related to the biologic rules and mathematical laws that control the growth and renewal of tissues in multi-cellular organisms that give rise to these patterns of Fibonacci numbers. Based on this asymmetric mechanism, our model output simulates the dynamic growth of cell populations and generation of hierarchical patterns found in tissues which are fluid, self-renewing, not stationary, cellular systems. Modeling asymmetric cell division also shows patterns of cell sub-populations based on cells having different temporal (not phenotypic) properties. Indeed, the plots and tables of model output illustrate that specific ratios of immature to mature cells emerge over time based on the cell maturation period. Specifically, the proportion of immature cells decreases as the maturation delay (c value) decreases. At a c value of one, the immature and mature cells would have identical kinetic properties and both would divide every cycle. Overall, our model suggests that simple mathematical laws involving temporal and spatial rules for cell division provide an explanation for how Fibonacci numbers appear in patterns of growth in nature.

The findings from our asymmetric cell division modeling likely has significance to stem cells in normal and cancer tissues. Stem cells are typically undifferentiated, slowly proliferating cells that reside in the stem cell niche in a tissue. Stem cells are responsible for production of the various lineages of differentiated cells and for tissue renewal. In this process, stem cells produce intermediate progenitor cells, termed transit amplifying (TA) cells, which are rapidly proliferating cells that differentiate into various specialized cell types. Since stem cells are the ones responsible for continuous tissue renewal, the population of stem cells must be maintained. But how stem cells maintain their numbers has not been fully clarified.

Previous studies have been done to understand the mechanisms that might regulate the proportion of stem cells in tissues. Two model mechanisms (deterministic and stochastic) have been proposed [8] as discussed below.

The deterministic model is based on asymmetric stem cell division. In this mechanism, stem cells are immortal and reside in the stem cell niche of a tissue. During cell division, each stem cell produces exactly one stem cell and one TA cell. The daughter stem cell continues to stay in the niche and the TA daughter cell migrates from the niche and continues to proliferate which leads to ongoing renewal of the tissue.

The stochastic model proposes that the niche contains several stem cells and each stem cell division produces two, one, or zero stem cells (or zero, one, or two TA cells, respectively). Because, over time, this leads to “drift” in number of descendants from each stem cell lineage, a single common ancestral stem cell will eventually become established from which all stem cells are descended. Based on the stochastic model, the likelihood that this stem cell population will persist depends on the probability that the production of either two stem cells, or zero stem cells, is equal.

In the “mating”-like design in the Spears and Bicknell-Johnson model [15, 16], stem cells are considered to be the replicating cells because these cells give birth to a new cell. This is likely due to the “mating”-like design whereby reproduction occurs after maturation (i.e. conception followed by gestation followed by reproduction). However, in biology stem cells are known to be undifferentiated and slowly proliferating cells rather than mature, rapidly dividing cells [2, 1]. In our cell division design, cell division occurs when immature cells reach maturity. If immature cells are considered to be stem cells, then mature replicating cells would be non-stem cells. In this case, cells would also have different degrees of stemness based on the c value and the cell’s stemness would decrease as the cell undergoes maturation. In this view, the rate of maturation would govern the proportion of stem cells or the degree of stemness in the cell population of a tissue.

6. CONCLUSION

Simple mathematical rules involving temporal and spatial rules for cell division, not just geometrical features, begin to explain how Fibonacci sequences appear in complex patterns of growth in nature such as tissue histology. These rules may help understanding how normal tissue renewal is disrupted. Therefore, diseases of aberrant tissue renewal such as cancer [3, 14, 13] can be better understood.

7. ACKNOWLEDGEMENTS

This research was supported in part by the Cancer Code Research Foundation and by a UNIDEL Graduate Research Fellowship. We thank the following students for their participation in various phases of this project: Matthew Saponaro, Kris Olli, Matt Schmittle, Nathaniel Borders, and Raghav Sambasivan.

Tables

Time	$c = 1$	$c = 2$	$c = 3$	$c = 4$	$c = 5$	$c = 6$
0	1	1	1	1	1	1
1	2	2	2	2	2	2
2	4	3	3	3	3	3
3	8	5	4	4	4	4
4	16	8	6	5	5	5
5	32	13	9	7	6	6
6	64	21	13	10	8	7
7	128	34	19	14	11	9
8	256	55	28	19	15	12
9	512	89	41	26	20	16
10	1024	144	60	36	26	21
11	2048	233	88	50	34	27
12	4096	377	129	69	45	34
13	8192	610	189	95	60	43
14	16384	987	277	131	80	55
15	32768	1597	406	181	106	71
16	65536	2584	595	250	140	92
17	131072	4181	872	345	185	119
18	262144	6765	1278	476	245	153
19	524288	10946	1873	657	325	196
20	1048576	17711	2745	907	431	251

TABLE 1. Number of cells as a function of maturation delay c .

Online Encyclopedia of Integer Sequences (OEIS) numbers	
$c = 1$	A000079
$c = 2$	A000045
$c = 3$	A000930
$c = 4$	A003269
$c = 5$	A003520
$c = 6$	A005708

TABLE 2. *

The insert above shows the Online Encyclopedia of Integer Sequences (OEIS) numbers that correspond to the sequences generated by our model based on asymmetric cell division in Table 1. Note that in Table 1 the maturation period for the clonogenic cell is not accounted for so that the first cell division starts at $n = 1$ in each case.

THE FIBONACCI QUARTERLY

Time	Generation											Total
	0	1	2	3	4	5	6	7	8	9	10	
0	1											1
1	1	1										2
2	1	2										3
3	1	3	1									5
4	1	4	3									8
5	1	5	6	1								13
6	1	6	10	4								21
7	1	7	15	10	1							34
8	1	8	21	20	5							55
9	1	9	28	35	15	1						89
10	1	10	36	56	35	6						144
11	1	11	45	84	70	21	1					233
12	1	12	55	120	126	56	7					377
13	1	13	66	165	210	126	28	1				610
14	1	14	78	220	330	252	84	8				987
15	1	15	91	286	495	462	210	36	1			1597
16	1	16	105	364	715	792	462	120	9			2584
17	1	17	120	455	1001	1287	924	330	45	1		4181
18	1	18	136	560	1365	2002	1716	792	165	10		6765
19	1	19	153	680	1820	3003	3003	1716	495	55	1	10946
20	1	20	171	816	2380	4368	5005	3432	1287	220	11	17711

TABLE 3. Number of cells per generation ($c = 2$).

PATTERNS OF GROWTH IN NATURE

Time	Generation											Total
	0	1	2	3	4	5	6	7	8	9	10	
0	1											1
1	1	1										2
2	1	2										3
3	1	3										4
4	1	4	1									6
5	1	5	3									9
6	1	6	6									13
7	1	7	10	1								19
8	1	8	15	4								28
9	1	9	21	10								41
10	1	10	28	20	1							60
11	1	11	36	35	5							88
12	1	12	45	56	15							129
13	1	13	55	84	35	1						189
14	1	14	66	120	70	6						277
15	1	15	78	165	126	21						406
16	1	16	91	220	210	56	1					595
17	1	17	105	286	330	126	7					872
18	1	18	120	364	495	252	28					1278
19	1	19	136	455	715	462	84	1				1873
20	1	20	153	560	1001	792	210	8				2745
21	1	21	171	680	1365	1287	462	36				4023
22	1	22	190	816	1820	2002	924	120	1			5896
23	1	23	210	969	2380	3003	1716	330	9			8641
24	1	24	231	1140	3060	4368	3003	792	45			12664
25	1	25	253	1330	3876	6188	5005	1716	165	1		18560
26	1	26	276	1540	4845	8568	8008	3432	495	10		27201
27	1	27	300	1771	5985	11628	12376	6435	1287	55		39865
28	1	28	325	2024	7315	15504	18564	11440	3003	220	1	58425

TABLE 4. Number of cells per generation ($c = 3$).

Time	Mature Cells	Immature Cells	Total
0	1	0	1
1	1	1	2
2	1	2	3
3	1	3	4
4	1	4	5
5	1	5	6
6	1	6	7
7	2	7	9
8	3	9	12
9	4	12	16
10	5	16	21
11	6	21	27
12	7	27	34
13	9	34	43
14	12	43	55
15	16	55	71
16	21	71	92
17	27	92	119
18	34	119	153
19	43	153	196
20	55	196	251

TABLE 5. Number of Mature & Immature cells ($c = 6$).

c value	M/I	Polynomial equation
1	1	
2	0.618034	$x^2 + x - 1 = 0$
3	0.465571	$x^3 + 2x^2 + x - 1 = 0$
4	0.380278	$x^4 + 3x^3 + 3x^2 + x - 1 = 0$
5	0.324718	$x^5 + 4x^4 + 6x^3 + 4x^2 + x - 1 = 0$
6	0.285199	$x^6 + 5x^5 + 10x^4 + 10x^3 + 5x^2 + x - 1 = 0$

TABLE 6. Ratio of Mature to Immature cells as a function of maturation delay c .

Figure Legends

Figure 1: Cell based model for asymmetric cell division where I = immature cell, M = mature cell, c = maturation delay.

Figure 2: Tree diagram from output of Agent-based Computer Code Model. Maturation Time $c = 6$, White = Clonogenic Cell, Red = Immature Cell, Blue = Mature Cell, Green = Wholly Mature Cell.

Figure 3: Tree diagram from output of Agent-based Computer Code Model. Maturation Time $c = 6$, $n_{wm} = n_{wm,0} - k$, $L = 50$, where $n_{wm,0} = 9$, White = Clonogenic Cell, Red = Immature Cell, Blue = Mature Cell, Green = Wholly Mature Cell.

Figures

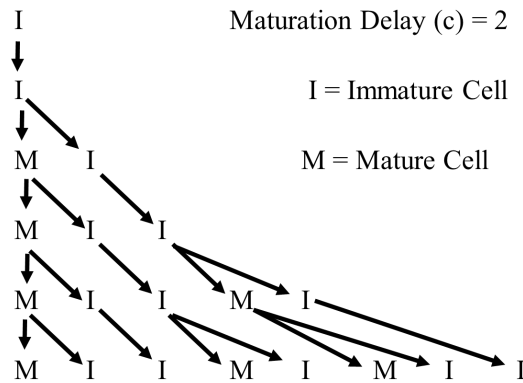


FIGURE 1. Cell based model for asymmetric cell division where I = immature cell, M = mature cell, c = maturation delay.

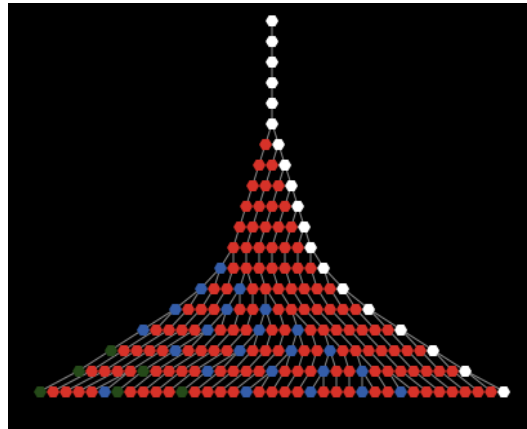


FIGURE 2. Tree diagram from output of Agent-based Computer Code Model. Maturation Time $c = 6$, White = Clonogenic Cell, Red = Immature Cell, Blue = Mature Cell, Green = Wholly Mature Cell.

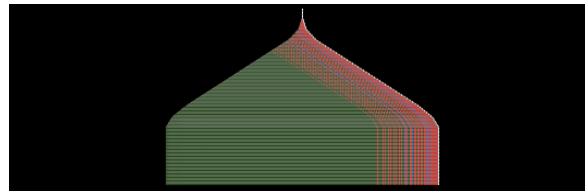


FIGURE 3. Tree diagram from output of Agent-based Computer Code Model. Maturation Time $c = 6$, $n_{wm} = n_{wm,0} - k$, $L = 50$, where $n_{wm,0} = 9$, White = Clonogenic Cell, Red = Immature Cell, Blue = Mature Cell, Green = Wholly Mature Cell.

REFERENCES

- [1] B. M. Boman, J. Z. Fields, K. L. Cavanaugh, A. Gujetter, and O. A. Runquist, *How dysregulated colonic crypt dynamics cause stem cell overpopulation and initiate colon cancer*, *Cancer Res.*, **6** (2008), 3304–3313.
- [2] B. M. Boman and M. S. Wicha, *Cancer stem cells: a step toward the cure*, *J. Clin. Oncol.*, **26** (2008), 2795–9.
- [3] L. Foulds, *Neoplastic Development*, volume 1, Academic Press, 1969.
- [4] R. Knott, (2010), Fibonacci numbers and nature, <http://www.maths.surrey.ac.uk/hosted-sites/R.Knott/Fibonacci/fibnat.html>
- [5] M. Livio, *The Golden Ratio: The Story of PHI, the World's Most Astonishing Number*, Random House, 2002.
- [6] J-C. Perez, *Codex Biogenesis - les 13 codes de l'ADN Broché*, Resurgence Editions Liège (Belgium), 2009.
- [7] J-C. Perez, *Deciphering hidden DNA meta-codes – the great unification & master code of biology*, *J Glycomics Lipidomics*, **5(2)** (2015).
- [8] S. Ro and B. Rannala, *Methylation patterns and mathematical models reveal dynamics of stem cell turnover in the human colon*, *Proc Natl Acad Sci USA*, **98** (2001), 10519–21.
- [9] D. S. Robertson, *Cellular configuration of DNA and cell division*, *Med Hypotheses*, **57(3)** (Sedt. 2001), 344–53.
- [10] M. H. Ross and W. Pawlina, *Histology: A Text and Atlas, with Correlated Cell and Molecular Biology*, LWW, 2015.
- [11] N. J. A. Sloane and S. Plouffe, *The Encyclopedia of Integer Sequences*, Academic Press, 1995.
- [12] N. J. A. Sloane, *A Handbook of Integer Sequences*, Academic Press, 1973.

- [13] C. Sonnenschein, A. M. Soto, A. Rangarajan, and P. Kulkarni, *Competing views on cancer*, J Biosci., **39(2)**, (Apr. 2014), :281–302.
- [14] C. Sonnenschein and A. M. Soto, *The Society of Cells: Cancer and Control of Cell Proliferation*, Springer Singapore, 1999.
- [15] C. P. Spears and M. Bicknell-Johnson, *Asymmetric cell division: Binomial identities for age analysis of mortal vs. immortal trees*, In G. E. Bergum, A. N. Philippou, and A. F. Horadam, editors, *Applications of Fibonacci Numbers 7*, pages 377–391. Springer Netherlands, 1998.
- [16] C. P. Spears, M. Bicknell-Johnson, and J. Yan, *Fibonacci phyllotaxis by asymmetric cell division: Zeckendorf and wythoff trees*, In F. Luca and P. Stanica, editors, *Congressus Numerantium 201*, pages 257–272, Winnepeg, Canada, 2009. Utilitas Mathematica Publishing.
- [17] A. Stakhov and S. Olsen, *The Mathematics of Harmony: From Euclid to Contemporary Mathematics and Computer Science*, World Scientific, 2009.
- [18] I. Stewart, *The Mathematics of Life*, Basic Books, 2011.
- [19] J. Wille, *Growth dynamics of individual clones of normal human keratinocytes: observations and theoretical considerations*, Natural Science, **3** (2011), 702–722.
- [20] J. Wille, *Occurrence of Fibonacci numbers in development and structure of animal forms: Phylogenetic observations and epigenetic significance*, Natural Science, **4** (2012), 216–232.

CENTER FOR APPLICATIONS OF MATHEMATICS IN MEDICINE, DEPARTMENT OF MATHEMATICAL SCIENCES, AND DEPARTMENT OF BIOLOGICAL SCIENCES, UNIVERSITY OF DELAWARE, NEWARK, DE 19716, AND CENTER FOR TRANSLATIONAL CANCER RESEARCH, HELEN F. GRAHAM CANCER CENTER & RES. INSTITUTE, NEWARK, DE 19713

E-mail address: bruceboman@gmail.com

DEPARTMENT OF COMPUTER AND INFORMATION SCIENCES, UNIVERSITY OF DELAWARE, NEWARK, DE 19716

E-mail address: tdinh@udel.edu

DEPARTMENT OF COMPUTER AND INFORMATION SCIENCES, UNIVERSITY OF DELAWARE, NEWARK, DE 19716

E-mail address: decker@udel.edu

DEPARTMENT OF MATHEMATICS, TRINITY COLLEGE, HARTFORD, CT 06106

E-mail address: brooks.emerick@trincoll.edu

CENTER FOR APPLICATIONS OF MATHEMATICS IN MEDICINE, DEPARTMENT OF MATHEMATICAL SCIENCES, UNIVERSITY OF DELAWARE, NEWARK, DE 19716

E-mail address: craymond@udel.edu

CENTER FOR APPLICATIONS OF MATHEMATICS IN MEDICINE, DEPARTMENT OF MATHEMATICAL SCIENCES, UNIVERSITY OF DELAWARE, NEWARK, DE 19716

E-mail address: schleini@udel.edu